Nie, S., MacCartney, G.R., Sun, S., Rappaport, T.S., 24th Annual IEEE International Symposium on Personal, Indoor and Mobile Radio Communications (PIMRC), Sept. 8~11, 2013.

72 GHz Millimeter Wave Indoor Measurements for Wireless and Backhaul Communications

Shuai Nie, George R. MacCartney Jr., Shu Sun, Theodore S. Rappaport
NYU WIRELESS
Polytechnic Institute of New York University, Brooklyn, NY 11201
tsr@nyu.edu

***Abstract*— As the mobile cellular carriers are currently facing a spectrum crunch, researchers are concentrating on higher carrier frequency bands, such as E-band (71-76 GHz and 81-86 GHz) for the next generation wireless communication systems. The E-band is promising due to its large available, continuous bandwidth and robust weather resilience. In this paper, we demonstrate a spread spectrum sliding correlator channel sounder operating at a center frequency of 73.5 GHz with an 800 MHz null-to-null bandwidth. The channel sounder provides a multipath time resolution of 2.33 ns. 72 GHz millimeter wave propagation and penetration characteristics in an indoor office environment are investigated using the sliding correlator channel sounding system. Data collected and processed from the measurements shows that strong received power can be achieved from the multipath-rich indoor environment, in the presence of multiple obstructions. The data obtained from this measurement campaign may be utilized for the design of future fifth generation millimeter wave indoor cellular systems.**

Keywords— E-band; 72 GHz; Millimeter Wave Communications; Channel Sounder; Sliding Correlator; Indoor Wireless; 5G

I. INTRODUCTION

The demand for greater bandwidths used in backhaul networks and mobile user applications drives the research for industry to meet and deliver dramatically higher data rates. For future application, millimeter wave (mm-wave) wireless transmission presents the ability to offer a large continuous bandwidth similar to fiber optic yet with lower cost and reduced infrastructure[1][2][3]. With the potential for gigabit-per-second throughput, the E-Band (71-76 GHz and 81-86 GHz) is abundant and adaptable for dense deployment, providing a major option for carrier-class wireless indoor and outdoor transmission.

A. Characteristics of E-band

E-band refers to the portion of electromagnetic spectrum between 70 GHz and 80 GHz, which is currently the highest frequency band used for commercial telecommunication networks [4]. The 5-10 GHz available bandwidths represent the most allocated spectra at any time, enabling fiber-like gigabit per second (Gbps) data rates, which cannot be realized in the band-limited lower microwave frequency bands. E-band can offer 1 Gbps and above, full-duplex throughput, extremely high data rates, and a cost-effective, fiber-like wireless solution. The E-band's large contiguous bandwidth along with other infrastructure advancements, will ensure the large data rates for the 10,000 fold increase in network capacity that is projected by 2025 [5]. E-band propagation characteristics are comparable to those of the widely used microwave bands, and rain attenuation characteristics are also known to be comparable to today's cellular bands for a microcellular environment of less than 200 meters [3][6][7]. Fig. 1 shows the atmospheric absorption in the mm-wave spectrum [3][6][7]. The propagation characteristics of E-band are only slightly worse than those of the widely used lower frequency bands. In the E-band range, atmospheric absorption is about 0.45 dB/km which translates to 0.09 dB / 200 meters. 200 meters inter-site distances are anticipated to be the industry standard for mm-wave, and atmospheric attenuation is practically negligible at this separation. Although at 60 GHz there are about 5 GHz license-free bandwidth, its strong atmospheric absorption makes 60 GHz not feasible for future outdoor-to-indoor communications, when compared to 72 GHz [8].

One of the challenges for E-band communication is to overcome higher path loss relative to legacy cellular bands. In free space, the path loss can be expressed as [9]

$$L_P = 32.4 + 20\log_{10} f + 20\log_{10} d \qquad (1)$$

where f is the center frequency in GHz and d is the distance in meters between a transmitter and receiver. For example, the free space path loss at 73.5 GHz is expected to be 8.38 dB greater than path loss at 28 GHz.

Although small obstructions will generate obvious attenuation effects in E-band communication links, with the deployment of highly directional steerable antennas, beamforming, a brand-new regime of E-band communication will be created to compensate for the extra path loss and attenuation.

B. E-band Millimeter Wave Regulations Worldwide

According to the International Telecommunication Union (ITU) Radio Regulations, the 71-76 GHz and 81-86 GHz bands are available for fixed and mobile services in all three ITU regions. In October 2003, the Federal Communications Commission (FCC) allocated the 71-76GHz, 81-86 GHz and 92-95 GHz bands to both federal government and non-federal government users on a co-primary basis, except the 94-94.1 GHz portion, which is allocated for exclusive federal government use [10]. Canada has adopted the same bands, with the same technical specifications and licensing regimens as the USA [11]. The UK Office of Communications (Ofcom)

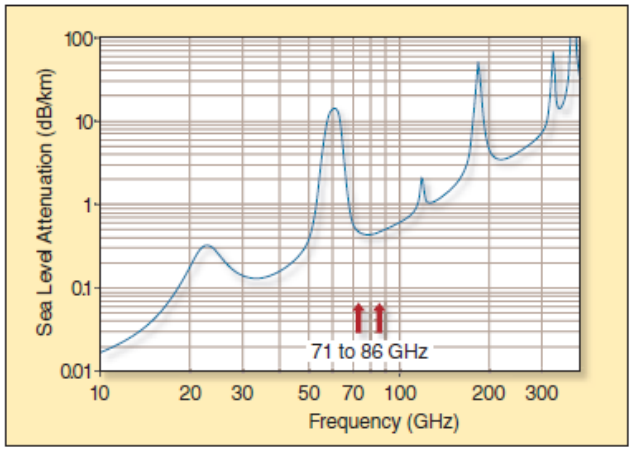

Fig. 1. Atmospheric absorption at mm-wave frequencies [3][4]. The attenuation of signal power caused by atmospheric absorption at 71 to 86 GHz is about 0.42 to 0.5 dB/km.

regulates UK communication industries and spectrum usage. It has responsibilities across television, radio, telecommunications and wireless services. In November 2006, Ofcom released a document to open the 71-76 GHz and 81-86 GHz bands for point-to-point broadband fixed wireless systems on a light licensed basis [12].

Australian Communications and Media Authority (ACMA) proposed a discussion paper in 2006 for planning the use of 71-76 GHz and 81-86 GHz mm-wave bands for wireless communications. The potential use of these mm-wave bands includes fiber point-of-present access, redundant access, enterprise campus connectivity, local area network (LAN) extension, local loop, metropolitan area network (MAN), wide area network (WAN) access, central office bypass, storage access, wireless backhaul, and high definition video, etc. The ACMA did not recommend any antenna use for 71-76 GHz communications [13].

Ireland is encouraging E-band adoption without the use of a light licensing procedure. Ireland licenses E-band links under its conventional fixed link methodology, which encourages the benefits that higher capacity radio systems bring [14].

C. *Previous Research Work in E-band*

Aalto University in Finland has conducted measurements and analyses of the mm-wave spectrum in the 60-90 GHz E-band range. Their research mainly focused on backhaul-to-backhaul scenarios, or point-to-point links. Kyro *et al.* were able to develop the structure for a delay domain channel model for mm-wave point-to-point applications in confined urban environments [15]. Researchers at Aalto University also studied 81-86 GHz channel characteristics by using a synthesizer sweeper as transmitter and a vector network analyzer as receiver. The measurement scenarios include street canyon and rooftop to street. Their results showed line-of-sight components dominantednyu the received signal, and multipath components were also observed [16]. Another long term path attenuation study under multiple weather conditions done by researchers at Ericsson Research in Sweden showed consistent attenuation results as predicted in ITU-R models [17]. However, little literature is found to carefully study multipath characteristics for both line-of-sight (LOS) and non-line-of-sight (NLOS) conditions in an indoor environment.

II. 72 GHz Sliding Correlator Channel Sounding System

A 400 Mega-chips per second (Mcps) spread spectrum sliding correlator channel sounder is developed to measure the 72 GHz radio channel for future backhaul and base station to mobile mm-wave communication systems. The channel sounding system uses state-of-the-art signal generators for an intermediate frequency (IF) at 5.625 GHz and a local oscillator (LO) frequency at 22.625 GHz. The 400 Mcps baseband PN sequence is first mixed with the IF to generate a spread spectrum IF signal. The LO frequency is tripled via a frequency tripler to 67.875 GHz in the upconverter, which then mixes the IF and LO to transmit the spread spectrum pseudorandom code at 73.5 GHz with an 800 MHz null-to-null RF bandwidth. This section presents the channel sounding system hardware.

A. *Sliding Correlator Description*

Table 1 shows the specifications of the 73.5 GHz sliding correlator channel sounding system, based on the theory developed by Donald Cox in [18]. The basic idea is to correlate two pseudo-random noise (PN) sequences at slightly different clock speeds at the transmitter and receiver, which results in a time dilation allowing small multipath resolution times [19]. The sliding correlator channel sounding system deployed in this measurement campaign can provide 2.33 nanoseconds multipath time resolution. In the future mm-wave communication regime, propagation delays will be measured on the order of tens of nanoseconds in order to have sufficient time resolution in a multipath-rich environment [20][21][22].

B. *Channel Sounder Equipment*

The block diagrams of the channel sounding system at both the transmitter and receiver are shown in Figs. 2 and 3, respectively. The baseband signal is a PN sequence with a chip rate of 400 Mcps. Currently the PN sequence is generated by a custom printed circuit board (PCB) [19]. In the future measurement campaign, the PCB will be replaced by a software controlled field-programmable gate array (FPGA) implementation. Instead of using a circuit board to generate a clock signal to drive the PN sequence generator, the channel sounding system uses the PXI-5652 signal generator, an exceptional RF and microwave signal generator produced by National Instruments. The signal generator can be remotely controlled by the PXIe-8135 embedded controller to generate the ideal clock signal. The PN sequence is then mixed with an intermediate center frequency of 5.625 GHz and passes through a controllable attenuator to adjust the output power level. The 5.625 GHz intermediate frequency is generated using the state-of-the-art QuickSyn Microwave Frequency Synthesizer provided by National Instruments. The frequency synthesizer provides low phase noise and fast switching speed

TABLE I. 73.5 GHZ SLIDING CORRELATOR CHANNEL SOUNDER SPECIFICATIONS

Carrier Frequency	73.5 GHz	Noise Floor	-80 dBm/Hz
Pseudorandom Code Chip Rate	400 Mcps	Maximum Measurable Path Loss	168 dB
RF Bandwidth (Null-to-Null)	800 MHz	Maximum Measurable Excess Delay	1800 ns
TX/RX IF Frequency	5.625 GHz	TX Antenna	27 dBi horn antenna 20 dBi horn antenna
TX/RX LO Frequency	22.625 GHz	RX Antenna	27 dBi horn antenna 20 dBi horn antenna
Multipath Delay Resolution	2.33 ns	Polarization	TX – Vertically polarized RX – Vertically and Horizontally polarized
Transmitter Power	12.3 dBm		

and can be controlled by a personal computer using a USB cable. The QuickSyn signal generator has greatly reduced the size and weight of the system that can be moved conveniently during future outdoor measurements. Another QuickSyn signal generator provides 11.3125 GHz signal that passes through a frequency doubler to create a 22.625 GHz local oscillator (LO) frequency. The upconverter triples the LO frequency and mixes the result with the IF signal to provide an output signal at a center frequency of 73.5 GHz (as shown in the blue box in Fig. 3). Three types of antennas are used for specific scenario measurements. For indoor measurements, a 20 dBi horn antenna (15° half power beamwidth) is connected by a WR-15 waveguide flange to the upconverter.

At the receiver side, an RF downconverter with the aforementioned antennas will be connected to receive a spread spectrum signal centered at 73.5 GHz. The received signal will be downconverted to a 5.625 GHz IF when mixed with a 67.875 GHz (22.625 GHz tripled LO) signal. The received IF signal power can be attenuated and amplified by a controllable attenuator, followed by a low noise amplifier, as shown in the block diagram in Fig. 4. After amplification, the IF signal will be demodulated to in-phase I and quadrature Q signal components [19]. A digitizer samples the I and Q signal components and the corresponding unprocessed power is recovered using National Instruments LabVIEW software, implemented to square and add the two voltage components $I^2 + Q^2$ to collect a power delay profile (PDP). The correlation is performed by a reference PN sequence at a slightly lower chip rate (399.95 Mcps) to create a slide factor of 8000. The PN sequence clock at the receiver side is also generated by a PXI-5652 signal generator.

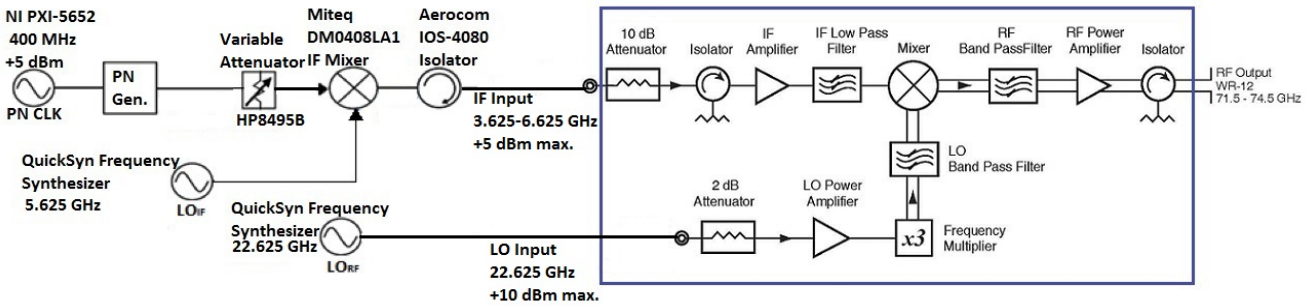

Fig. 2 Block Diagram of the Sliding Correlator Channel Sounding System at Transmitter Side

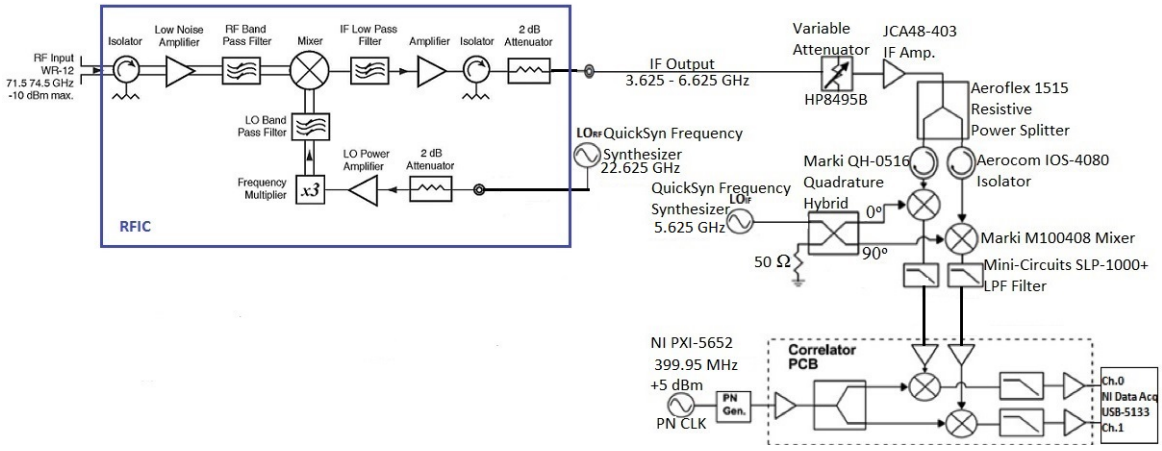

Fig.3 Block Diagram of the Sliding Correlator Channel Sounding System at Receiver Side

III. 72 GHz Indoor Measurement Procedure

The E-band indoor measurement campaign includes multiple penetration measurements. The indoor measurements result in propagation characteristics at 72 GHz in a typical office area, and will help in determining the viability of the 72 GHz band as a solution to indoor, broadband, and high data rate applications similar to the use of 60 GHz. These measurements may eventually be in high demand of Gbps WiFi routers that will operate in the 72 GHz frequency range. Penetration tests allow for learning about the penetration losses and penetration coefficients of common barriers in the office environment such as cubicles and walls.

The indoor measurements were performed on the 9th floor of 2 MetroTech center in Brooklyn, New York. The transmitter location is in the center of an open office area. Eleven receiver locations were selected behind cubicles, walls, and common office obstructions. A pair of 20 dBi gain antennas (15° half-power beamwidth) was used at the transmitter (TX) and receiver (RX) locations. The heights of TX and RX antennas are both 1.61 meters. As shown in Fig. 4, RX 1 and 6 are behind one cubicle wall, RX 2, 5, 7 and 9 are behind two cubicle walls with different TX-RX separation distances. RX 3 is behind three cubicle walls. RX 4, 8, 10 and 11 are located behind multiple cubicles and dry walls. The widths of each cubicle wall and dry wall are 2.5 cm and 13 cm, respectively. TX and RX separation distances are shown in Table 2. The smallest separation distance from the TX was to RX 1, 6.8 m. The largest separation distance from the TX was to RX 10 and 11, 15.2m.

At the beginning of measurements, a five meter free space calibration routine was performed to find the true free space received power levels. Then the TX and RX antennas were separated at specific distances (as shown in Table 2) behind obstructions. Both the antennas were pointed directly at each other (boresight to boresight), as the paths shown in Fig. 4. Power Delay Profiles (PDPs) were also collected to study the multipath of each location.

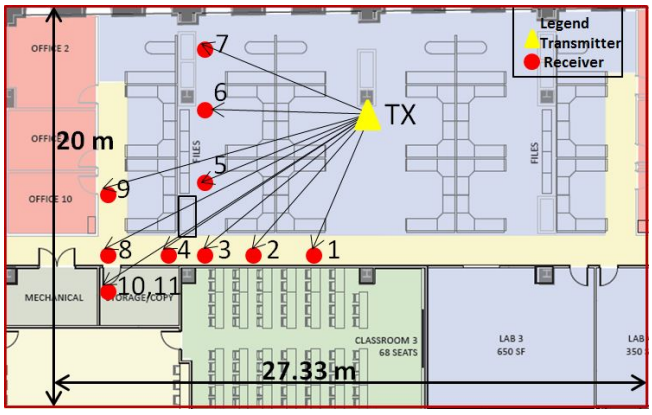

Fig. 4 Indoor penetration measurements at 2 MTC 9th floor. The TX location is marked by a yellow star, the RX locations are shown as red dots. The paths for signal penetration are shown with black arrows.

IV. 72 GHz Indoor Penetration Analysis

Table 2 contains the penetration loss values of multiple obstructions (including cubicle walls, dry walls and wood doors) in a typical office environment, with various TX-RX separation distances and different numbers of partitions illustrated in Fig. 4.

As shown in Fig. 4 and Table 2, there is no definite relationship between the penetration loss and the distance of the TX and RX. For example, the separation distance for RX 7 is 8.8 m, which is 4.2 m less than that for RX 9, and the number and material of obstructions are the same for these two RX locations, but RX 7 has a much larger penetration loss than RX 9. Further, heavier obstructions do not necessarily result in more penetration loss. Although RX 8 is blocked by three cubicle walls, one wood door, and a dry wall closet from the TX, RX 4 is only blocked by two cubicle walls, one wood door and one dry wall, and the separation distance is smaller than that between the TX and RX 8, although the penetration loss at RX 4 is significantly greater compared to RX 8. This phenomenon can be attributed to multipath caused by reflections, and the fact that the boresight of the antenna at RX 4 was less than 20 cm from the dry wall. This would make it difficult for the RX 4 measurement to capture a large amount of energy in such a narrow beamwidth. In addition, the transmitted signal may be reflected several times by the dry wall, cubicle wall, and the wall of Classroom 3 (see Fig. 4), and is eventually received by RX 8. For RX 4, however, after multiple reflections, part of the signal did not propagate into the narrow beamwidth of the receiver at RX 4, thus the received power is much lower. The results can be confirmed by the PDPs at RX 4 and RX 8, as showed in Fig. 5. More multipath components are obtained at RX 4, but both the individual power of each multipath component and the total power are much lower than those at RX 8. The results above indicate that the received power may vary greatly for different indoor RX locations separated by 2~3 meters, depending on the specific topography of the surrounding environment. Therefore, the TX locations should be adjusted according to the RX position topology.

TABLE II. Penetration Losses at Different Receiver Locations at 73.5 GHz . Numbers and Types of Obstructions are Listed. Both of the Transmit and Receive Antennas are 20 dBi Gain with 15° Half-power Beamwidth. The RX ID Numbers Correspond to the Locations Labeled in Fig. 4. Multiple Obstructions Existed between TX and RX.

RX ID	TX-RX Separation (m)	# of Partitions				Received Power for Free Space (dBm)	Received Power for Test Material (dBm)	Penetration Loss (dB)
		Cubicle Wall	Metal Cabinet	Dry Wall	Wood Door			
1	6.8	1	0	0	0	-34.1	-39.4	5.3
2	8.0	1	1	0	0	-35.6	-52.8	17.2
3	10.1	2	2	0	0	-37.6	-61.4	23.8
4	11.5	1	2	1	1	-38.7	-75.5	36.8
5	8.6	0	2	0	0	-36.2	-50.3	14.1
6	8.1	0	2	0	0	-35.7	-45.4	9.7
7	8.8	1	2	0	0	-36.4	-63.0	26.6
8	14.0	0	2	1	1	-40.4	-55.6	15.2
9	13.0	1	3	0	0	-39.7	-53.0	13.3
10	15.2	1	2	1	0	-41.1	-60.4	19.3
11	15.2	1	2	1	0	-41.1	-59.0	17.9

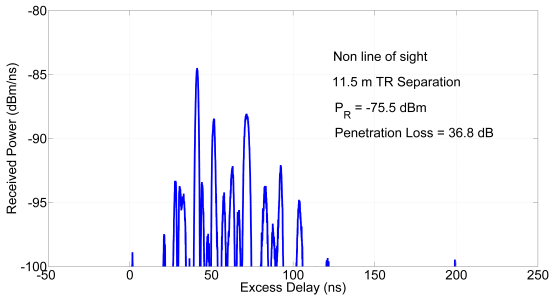

(a)

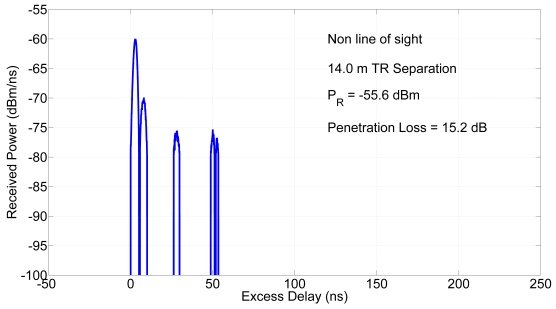

(b)

Fig.5 Multipath delay spread observed at (a) RX 4 and (b) RX 8 in the penetration measurements on 9th floor, 2 MTC at 73.5 GHz. P_R is the total received power at each RX location.

V. CONCLUSION

This paper presents the features of E-band and its potential applications in future mm-wave cellular communications. A channel sounder is developed to afford a 2.33-ns multipath time resolution utilizing mechanically steerable horn antennas. Thus far, measurement results show the viability of the 72 GHz mm-wave band for indoor WiFi Gbps applications. The penetration losses measured are not significantly different than those for current WiFi. The channel sounding system will be employed in further indoor measurements for four different scenarios that will yield significant statistics of mm-wave radio propagation. With these measurements, analyses will be done to build a robust statistical spatial channel model for E-band frequencies.

ACKNOWLEDGMENT

This work is sponsored by Nokia Siemens Network (NSN), National Instruments (NI), and the GAANN Fellowship Program. The authors wish to thank Amitava Ghosh of NSN, Ahsan Aziz of NI, and Mathew Samimi and Hannar J. Lee of NYU WIRELESS for their support and contributions to this project. Measurements were and will be recorded under U.S. FCC Experimental License 0040-EX-ML-2012.

REFERENCES

[1] T. S. Rappaport, S. Sun, R. Mayzus, H. Zhao, Y. Azar, K. Wang, G. N. Wong, J. K. Schulz, M. Samimi, F. Gutierrez, "Millimeter WaveMobile Communications for 5G Cellular: It Will Work!", IEEE Access (Invited), Vol. 1, No. 1, pp. 335~349, May 2013.

[2] T. S. Rappaport, F. Gutierrez, E. Ben-Dor, J. N. Murdock, Y. Qiao, J. I. Tamir, "Broadband Millimeter-Wave Propagation Measurements and Models Using Adaptive-Beam Antennas for Outdoor Urban Cellular Communications", IEEE Transactions on Antennas and Propagation, Vol. 61, No. 4, pp. 1850~1859, April 2013.

[3] T. S. Rappaport, J. N. Murdock, F. Gutierrez, "State of the Art in 60-GHz Integrated Circuits and Systems for Wireless Communications", Proceedings of the IEEE, Vol. 99, No. 8, pp. 1390~1436, August, 2011.

[4] J. A. Wells, "Faster than fiber: The future of Multi-Gb/s wireless", IEEE Microwave Magazine, vol.10, No.3, pp.104~112, May 2009.

[5] Nokia Siemens Network White Paper, "2020: Beyond 4G Radio Evolution for the Gigabit Experience".

[6] J. Wells, "Multigigabit wireless technology at 70 GHz, 80 GHz and 90 GHz," available at http://rfdesign.com/mag/605RFDF4.pdf.

[7] Q. Zhao; J. Li; "Rain Attenuation in Millimeter Wave Ranges," Inter. Symp. on Antennas, Propagation & EM Theory, Oct. 26~29, 2006.

[8] H. Xu, V. Kukshya, T. S. Rappaport, "Spatial and Temporal Characteristics of 60-GHz Indoor Channels", IEEE Journal on Selected Areas in Communications, vol. 20, No. 3, pp. 620~630, August, 2002.

[9] M. Marcus, B. Pattan, "Millimeter Wave Propagation Spectrum Management Implications", IEEE Microwave Magazine, vol. 6, No. 2, pp. 54~62, Jun. 2005 (FCC Office of Engineering and Technology Bulletin Number 70, Jul. 1997).

[10] FCC 03-248, "Allocation and Service Rules for the 71-76GHz, 81-86GHz and 92-95GHz Bands", Federal Communication Commission, Nov. 2003.

[11] DGTP-001-05,"Consultation on a renewed spectrum Policy Framework for Canada and Continued Advancement in Spectrum Managements", Sep. 2005.

[12] Ofcom "Making Spectrum Available for the 71-78 GHz and 81-86 GHz Bands", Nov. 2006.

[13] ACMA, Planning of the 71-76 GHz and 81-86 GHz Bands for Millimeter Wave High Capacity Fixed Link Technology, Spectrum Planning Discussion Paper Nov. 2006.

[14] "Revised Guidelines to Applicants for Radio Links - Point-to-Point above 1GHz Licenses," Document 98/14R5, 28 December 2007.

[15] M. Kyrö, et al., "Experimental Propagation Channel Characterization of mm-Wave Radio Links in Urban Scenarios," IEEE Antennas and Wireless Propagation Letter, Vol. 11, pp. 865~868, Aug. 2012.

[16] M. Kyrö, S. Ranvier, V. Kolmonen, K. Haneda, and P. Vainikainen, "Long Range Wideband Channel Measurements at 81-86 GHz Frequency Range", 2010 Proceedings of the Fourth European Conference on Antennas and Propagation (EuCAP), April 12~16, 2010.

[17] J. Hansryd, Y. Li, J. Chen, and P. Ligander, "Long Term Path Attenuation Measurement of the 71-76 GHz Band in a 70/80 GHz Microwave Link", 2010 Proceedings of the Fourth European Conference on Antennas and Propagation (EuCAP), April 12~16, 2010.

[18] D.C. Cox, "Delay Doppler Characteristics of Multipath Propagation at 910 MHz in a Suburban Mobile Radio Environment," IEEE Trans. On Ant. and Prop., vol. Ap-20, No. 5, pp. 625~635, Sept. 1973.

[19] E. Ben-Dor, T.S. Rappaport, Y. Qiao, S. Lauffenburger, "Millimeter-wave 60 GHz Outdoor and Vehicle AOA Propagation Measurements using a Broadband Channel Sounder,"IEEE Global Telecommunications Conference (GLOBECOM 2011), pp. 1~6, Dec. 2011.

[20] H. Zhao, R. Mayzus, S. Sun, M. Samimi, J. K. Schulz, Y. Azar, K. Wang, G. N. Wong, F. Gutierrez, Jr., T. S. Rappaport, "28 GHz Millimeter Wave Cellular Communication Measurements for Reflection and Penetration Loss in and around Buildings in New York City", 2013 IEEE International Conference on Communications (ICC), June 9~13, 2013.

[21] Y. Azar, G. N. Wong, K. Wang, R. Mayzus, J. K. Schulz, H. Zhao, F. Gutierrez, Jr., D. Hwang, T. S. Rappaport, "28 GHz Propagation Measurements for Outdoor Cellular Communications Using Steerable Beam Antennas in New York City", 2013 IEEE International Conference on Communications (ICC), June 9~13, 2013.

[22] M. Samimi, K. Wang, Y. Azar, G. N. Wong, R. Mayzus, H. Zhao, J. K. Schulz, S. Sun, F. Gutierrez, Jr., T. S. Rappaport, "28 GHz Angle of Arrival and Angle of Departure Analysis for Outdoor Cellular Communications using Steerable Beam Antennas in New York City," 2013 IEEE Vehicular Technology Conference (VTC), June 2~5, 2013.